JET-R(96)09

Comments on X-point Dynamics and ELMs

F Porcelli.

JET Joint Undertaking, Abingdon, Oxfordshire, OX14 3EA, UK.

ABSTRACT

Current sheets can develop spontaneously in the vicinity of magnetic X-points. It is argued that current sheet formation in a Tokamak configuration may be related to a non-rigid vertical displacement of the resistive plasma, which peaks near the X-point. The relevance of this process to the understanding of ELMS is discussed.

1. INTRODUCTION

Edge localised modes (ELMs) are a persistent feature of Tokamak configurations which include a magnetic X-point [1-3]. These modes lead to a degradation of the plasma confinement and are often associated with the termination of high performance discharges. However, the instability mechanism is still rather obscure. There is a clear need to develop a theoretical model which can suggest effective means of instability control, and on which basis realistic plasma transport simulations can be performed. Although there is ample evidence that the ELM instability is associated with the presence of magnetic X-points, there have been very few theoretical efforts [4] within the Tokamak community devoted to the understanding of specific X-point MHD effects. This situation is somewhat anomalous, especially in view of the predominant position that divertor physics studies occupies at present within the world wide magnetic fusion programme.

The purpose of this note is to address some specific X-point effects that may be relevant to the understanding of ELMs. It is argued that vertical plasma displacements, which are normally suppressed by the feedback stabilisation system in elongated Tokamak configurations, may reappear in the form of a fast, non-rigid, vertical displacement which affects mostly the peripheral plasma region near the magnetic X-point. The vertical displacement has a spatial structure which is dominated by the n=0, m=1 toroidal and poloidal mode numbers. The parallel wave vector,

$$\mathbf{k}.\mathbf{B} = nB_{\varphi} / R + mB_{\vartheta} / r \qquad (1)$$

vanishes at the X-point for n=0. Therefore, the presence of the X-point is essential in that it allows for a non-rigid vertical displacement which peaks near the X-point, thus minimising magnetic field line bending. The structure of this mode is reminiscent of that of an ordinary tearing mode.

Let us first list some basic experimental facts on ELMs at JET. These are drawn from Refs. 2, 3 and are limited to the so-called [1] type I, or giant ELMs.

i) Magnetic diagnostics indicate that during the ELM the plasma current centroid shifts downwards by about 1 cm, reaching its lowest position in several hundred microseconds.

This rapid downward motion is followed by a slower upward shift, possibly due to the response of the feedback stabilisation system;

ii) The dominant mode structure is m=1, n=0;

iii) Infra-red camera data on the divertor target show an increase in the strike zone separation during the ELM by tens of centimetres. This increase is too large to be the result of the measured plasma bulk movement, therefore the existence of SOL currents is suggested;

iv) This is supported by Langmuir probe measurements of SOL currents intercepted by the divertor target during ELMs.

v) X-ray data indicate a rapid increase of emission in the divertor region, over a time scale of ~20μs, possibly due to non thermal electrons. Since this time scale is much shorter than that measured by magnetic diagnostics, as indicated in point (i) above, it may suggest a two-stage process.

2. X-POINTS AND CURRENT SHEETS

X-points are special points of a two-dimensional field where a component of the magnetic field vanishes. Near the X-point the field structure is hyperbolic in nature. The field lines that pass through the X-point form the separatrix. If the X-point lies in vacuum, then the angles at the separatrix are 90° angles. Consider, for instance, a field representation of the type $\mathbf{B} = B_\varphi \mathbf{e}_\varphi + \mathbf{e}_\varphi \times \nabla\psi$, where ψ is the flux function and axisymmetry is assumed ($\partial/\partial\varphi = 0$; φ is the toroidal angle). It follows that

$$(\nabla \times \mathbf{B})_\varphi = \left(\nabla^2 \psi\right)\mathbf{e}_\varphi = \frac{4\pi}{c} J_\varphi \mathbf{e}_\varphi \qquad (2)$$

Thus, if $J_\varphi = 0$ at the X-point, then $\nabla^2\psi = 0$ implies that locally $\psi = (B'_{xo}/2)\ (x^2-y^2)$, where x and y are Cartesian coordinates centred at the X-point (see Fig. 1a), and B'_{xo} is the slope of B_x at the X-point.

The X-point is a weak spot in the magnetic field structure in the sense that the motion of distant sources can make the field near such a point collapse into a current sheet whose width is limited by resistive diffusion. Such process has been studied extensively, especially in the context of astrophysical plasmas [5,6]. When a current sheet forms, the resulting magnetic structure is such that the X-point splits into two Y-points as shown in Fig. 1b. In the limit of small resistivity, the distance between the two Y-points should be approximately equal to the length of the current sheet. This configuration corresponds to a force-balance equilibrium, with $J_\varphi = J_\varphi(\psi)$ and resistive diffusion in the sheet region sustained by plasma flow into that region. In actual fact, the current sheet should extend in narrow layers along the arms of the ψ = constant separatrix.

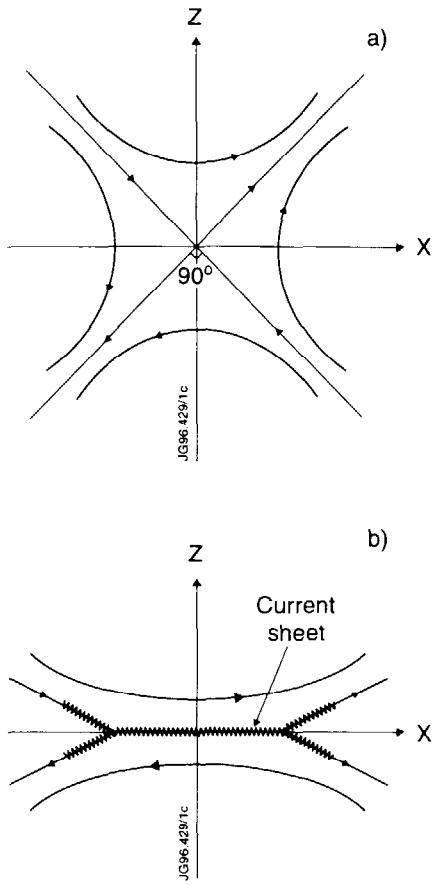

Fig.1: ψ = constant magnetic flux surfaces. (a) Hyperbolic topology near a magnetic X-point in the currentless case. The separatrix line forms 90° angles. (b) Double-Y magnetic topology in the presence of a current sheet.

In the following, a back-of-the-envelope calculation indicates the order of magnitude of the current in the X-point region of a JET plasma that is necessary in order to account for the observed increase in the strike zone separation on the divertor target plates during ELMs. With reference to Fig. 2, for the sake of simplicity both the plasma current and the currents in the divertor coils are modelled by two wires, carrying respectively the currents I_p = 3 MA and I_D = 1 MA. The resulting X-point with 90° angles and relative distances from the current wires are indicated in the figure. The target plates are located below the X-point at a minimum distance of 10 cm.

We introduce the Cartesian coordinates x, z with origin at the X-point. Then, we add a narrow current sheet having the functional form

$$J_x = (I_x/2\Delta)\, \delta(z)\, H\, (\Delta^2 - x^2) \qquad (3)$$

where H(x) is the unit step function, Δ is the half-width of the current sheet and I_x is the total current in the sheet. As shown in Fig. 3, we find that values of I_x = - 100 KA and Δ = 5 cm

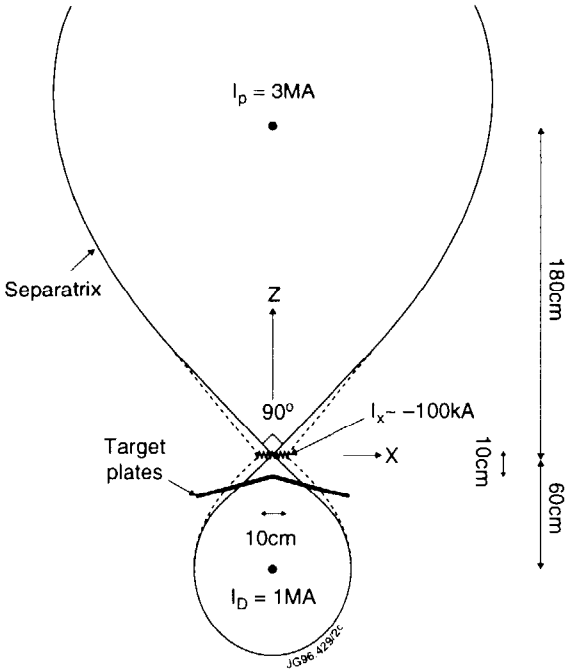

Fig.2: Plasma and divertor current "wires", modelling a typical JET case. The position of the divertor target plates relative to the equilibrium X-point is indicated. The dashed curves sketch the local change in the flux surfaces when an X-point current is added, with I_X ~ - 100 kA and sheet length ~10cm.

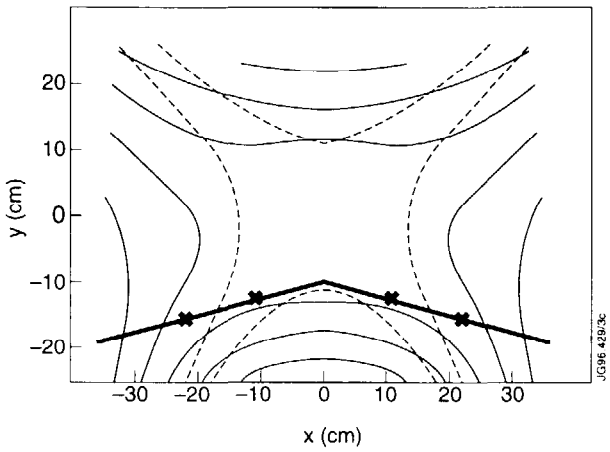

Fig.3: Blow up of the flux contours near the equilibrium. The strike points at the target plates are indicated by crosses. A current sheet with a length of 10cm and a current I_X = - 100 kA has been considered. The dashed curves indicate the position of the separatrix prior to the introduction of the current sheet. An outward shift of the strike points by about 11 cm on each target plate is clearly visible.

cause an outward displacement of the strike points on each divertor plate by about 11 cm. Note that I_X is negative with respect to the plasma and divertor currents.

As remarked earlier, the actual situation is somewhat more complicated. The current sheet will extend along the double-Y separatrix line and will intercept the target plates, where it can be measured by Langmuir probes. As a dynamic process, the formation of a current sheet will induce image currents over nearby metallic surfaces and the whole plasma may move. Nevertheless, this back-of-the-envelope calculation shows that relatively small localised currents, on the order of 100 KA, may be sufficient to account for the observed shift of the strike points, without any need for significant bulk plasma movements.

3. MECHANISM FOR THE FORMATION OF A CURRENT SHEET IN THE X-POINT REGION OF A TOKAMAK PLASMA.

In this Section, we argue that ELMs are initiated by a non-rigid, resistive vertical displacement, whose structure resembles that of a tearing mode localised in the X-point region. The argument is based on two basic points:

i) The vertical displacement, dominated by the n = 0, m = 1 mode-numbers, is resonant at the X-point, in the sense that the parallel wave-vector vanishes there (see Eq. 1);

ii) The resonant nature allows for a non-rigid displacement which peaks in the X-point region. As a by product, the plasma current centroid is not significantly displaced, while an X-point current sheet grows on a local resistive time scale which is shorter than the response time of the feedback stabilisation system.

To present our argument more clearly, first the dynamics of vertical displacements in elongated plasmas [7] is reviewed briefly in the next two sub sections. In the absence of magnetic X-points, the vertical instability corresponds to a rigid plasma shift. This allows for a simplified electro-mechanical model of the vertical instability [8]. In the realistic case of a plasma inside a metallic chamber, the rigid vertical displacement normally grows on the time scale of the resistive penetration time of the wall. Of course, this rigid, resistive vertical instability in a Tokamak is suppressed by the feedback stabilisation system.

A. Electro-mechanical model for the vertical instability: the ideal limit

Let us consider the equilibrium of three current wires as shown in Fig. 4. At equilibrium, the "plasma wire" carrying the current I_p is located at z = 0, while the two equal divertor currents, I_D, are located at z = ± d. The divertor wires are fixed in space, while the plasma wire is free to move along the z direction. Vacuum is assumed to surround the three wires, thus no current through the X-points is allowed (for convenience, we consider here a double-null magnetic configuration instead of the single-null divertor geometry typical of JET; this simplifying assumption does not change the qualitative behaviour described below).

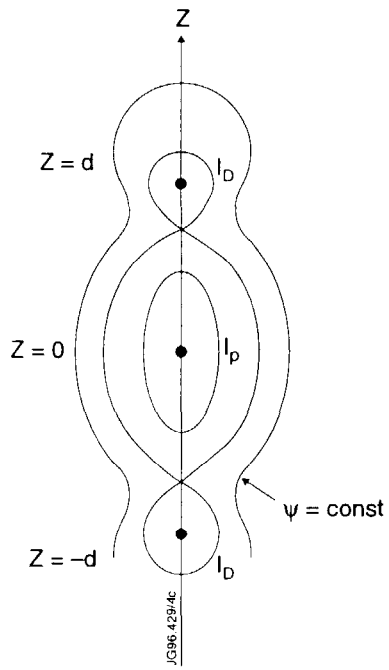

Fig.4: Schematic equilibrium of three current wires.

The equation of motion for the plasma wire is (in c.g.s. units)

$$\mu\ddot{z} = \frac{4I_pI_D}{c^2}\,\frac{z}{d^2 - z^2} \qquad (4)$$

where μ is the linear plasma mass density. We neglect self and mutual induction currents. Thus, I_p and I_D remain constant as the plasma wire is displaced. For small z<<d, the solution of Eq. (4) is

$$z = z_0 e^{t/\tau_{in}} \tag{5}$$

where z_0 is an initial displacement and

$$\tau_{in} = \left(\frac{\mu c^2}{4 I_p I_D}\right)^{1/2} d \approx \frac{1}{2}\left(\frac{I_p}{I_D}\right)^{1/2} \tau_A \tag{6}$$

is an "inertial" time, with τ_A the Alfvén time based on the current I_p and the distance d. Thus, the equilibrium of Fig. 4 is unstable, with an instability growth time represented by τ_{in}. For typical JET parameters, τ_{in} ~ 1 μs.

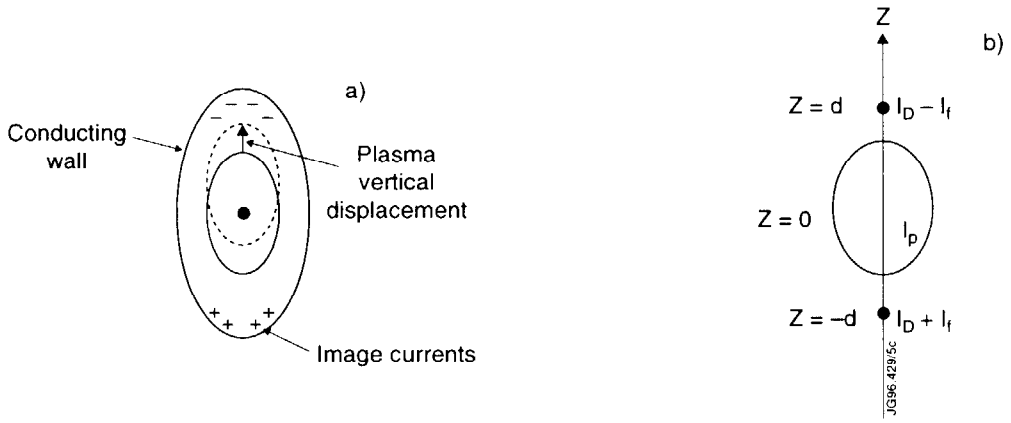

Fig.5: Effect of a conducting wall on rigid vertical displacements of the plasma. (a) Image currents are induced on the conducting wall. (b) The image current can be modelled by two currents of opposite sign, ± I_f, localised at z = ∓d.

This "ideal" vertical instability is suppressed in the presence of a perfectly conducting wall provided this wall is not too far away from the plasma. When the plasma is displaced from its equilibrium position, image currents are induced at the wall, see Fig. 5a. The sign of these currents is such that the corresponding force opposes the plasma motion. The effect is equivalent to that of two currents of opposite sign, ± I_f, localised at the same spatial positions as the divertor currents, as shown in Fig. 5b. The currents ± I_f are driven by an induced e.m.f. proportional to ż. Thus, in the perfectly conducting limit, we can write the equation for the induced currents,

$$L\dot{I}_f = V_f = DLI_D \dot{z} / d \tag{7}$$

where L is an effective inductance and D is a dimensionless proportionality constant which in the actual problem depends on the plasma and wall geometry.

Including the effect of the image currents modelled by $\pm I_f$, with I_f solution of Eq. (7), the equation of motion for the plasma wire becomes

$$\mu\ddot{z} = 4I_pI_D\frac{z}{d^2 - z^2} - 4I_pI_f\frac{d}{d^2 - z^2} \tag{8a}$$

$$= 4I_pI_D(1 - D)z / d^2 \tag{8b}$$

where in the last equation we have taken z<<d. Thus, stability is obtained for

$$D > 1 \tag{9}$$

In this limit, a displacement of the plasma from its equilibrium position results in a oscillatory motion with a characteristic frequency

$$\omega_0 = (1 - D)^{1/2}\tau_{in}^{-1} \tag{10}$$

The geometrical factor D can be computed analytically for the case of confocal elliptical plasma and wall cross-sections and uniform plasma current distribution [7]:

$$D = \frac{b + a}{b - a}\left(\frac{b + a}{b_w + a_w}\right)^2 \tag{11}$$

where (a, b), (a_w, b_w) are the minor and major axis of the plasma and wall elliptical cross sections, respectively.

The ideal stability criterion (9) is certainly satisfied in well designed Tokamaks with shaped cross-sections.

B. The resistive case

Assuming ideal stability, D > 1, vertical displacements may still grow in time in the more realistic case of a resistive wall. In our simple electromechanical model, we can add a resistive term to Eq. (7) for I_f, so to obtain

$$RI_f + L\dot{I}_f = DLI_D\dot{z} / d \tag{12}$$

Taking the time derivative of Eq. (8a), we obtain for z<<d

$$\mu\dddot{z} = \left(4I_pI_D / d^2\right)\dot{z} - \left(4I_p / d\right)\dot{I}_f \tag{13}$$

Eliminating $\dot{I}_f$ using Eq. (12) and I_f using Eq. (8a), we find the third order equation for z(t):

$$\dddot{z} + \frac{1}{\tau_R}\ddot{z} + \omega_0^2\dot{z} - \frac{1}{\tau_R}\frac{\omega_0^2}{(D-1)}z = 0 \tag{14}$$

where we have introduced the effective "resistive wall penetration time", $\tau_R = L/R$.

Looking for solutions $z(t) \sim e^{\gamma t}$, we obtain the dispersion relation

$$\gamma^3 + \frac{1}{\tau_R}\gamma^2 + \omega_0^2\gamma - \frac{\omega_0^2}{(D-1)\tau_R} = 0 \tag{15}$$

With D given by Eq. (9), this dispersion relation agrees very well with that of Wesson [8]. In fact, the agreement is complete if we renormalise the plasma mass density as $\mu \rightarrow (1-s^2)\mu$, where the geometrical factor $s = (a + b)/(a_w+b_w) < 1$.

Let us consider the limit of small resistivity, $\omega_0\tau_R >> 1$. In this limit, we find that the two oscillatory solutions of the ideal case are both damped by resistivity,

$$\omega \approx \pm\omega_0 - \frac{iD}{2(D-1)\tau_R} \tag{16}$$

where $\omega \equiv -i\gamma$. The third root, however, corresponds to a purely growing resistive instability, with a growth rate

$$\gamma \approx \frac{1}{(D-1)\tau_R} \tag{17}$$

A typical value of the resistive wall penetration time at JET is $\tau_R \sim 5$ ms. Over this time scale, the feedback stabilisation system acts to suppress the resistive vertical instability. Indeed, the typical response time of this system at JET is of the order of 1 ms. The system responds to displacements of the plasma current centroid as measured by magnetic diagnostics [9].

So far, we have considered an ideal plasma and a resistive wall. Qualitatively, we would have reached a similar conclusion if we considered instead a resistive plasma and a perfectly conducting wall. In this case, the plasma can diffuse across the field lines and it would reach the wall over a time scale of the order of the global plasma resistive time,

$$\tau_\eta \sim 4\pi b^2 / \eta c^2 \tag{18}$$

where η is the mean plasma resistivity (c.g.s. units!). However, in a hot fusion plasma, this time is normally much longer than τ_R.

The simple electro-mechanical model reproduces very well the qualitative features of the dynamics of vertical plasma displacements. There is a simple reason for this: the actual plasma

displacement, solution of the Euler-Lagrange plasma equations, corresponds to a rigid plasma shift, which minimises the restoring force associated with magnetic field line bending. In other words, non-rigid vertical displacements are energetically more costly. This statement is true, however, only insofar as the plasma does not extend to the magnetic X-point.

C. X-points and non-rigid displacements

Let us discuss the possibility of modes that grow on a time scale shorter than the resistive wall penetration time, τ_R. Therefore, let us consider again a perfectly conducting wall and a resistive plasma. This time, however, we assume that the plasma extends to the separatrix magnetic surface. As we remarked earlier, the n=0, m=1 vertical displacement is resonant at the X-point. Since this displacement is ideally stable because of the presence of the ideal wall, it tends to become divergent at the X-point in the limit of negligible plasma resistivity. A finite resistivity resolves the singularity, giving rise to a mode structure which peaks near the X-point, as shown in Fig. 6a. Note that the vertical displacement is rigid although relatively small almost up to the X-point. Thus, the plasma current centroid (the magnetic axis) will undergo an observable, albeit small displacement. Nevertheless, most of the motion will occur near the X-point, where the non-rigidity of the displacement is localised. The displacement vector will include both z and y components, and assuming incompressibility two vortex cells will form. Figure 6b shows an example of such cells. There will also be weaker global cells that set the magnetic axis in motion, however the recirculating time of these cells is much longer than those localised near the X-point.

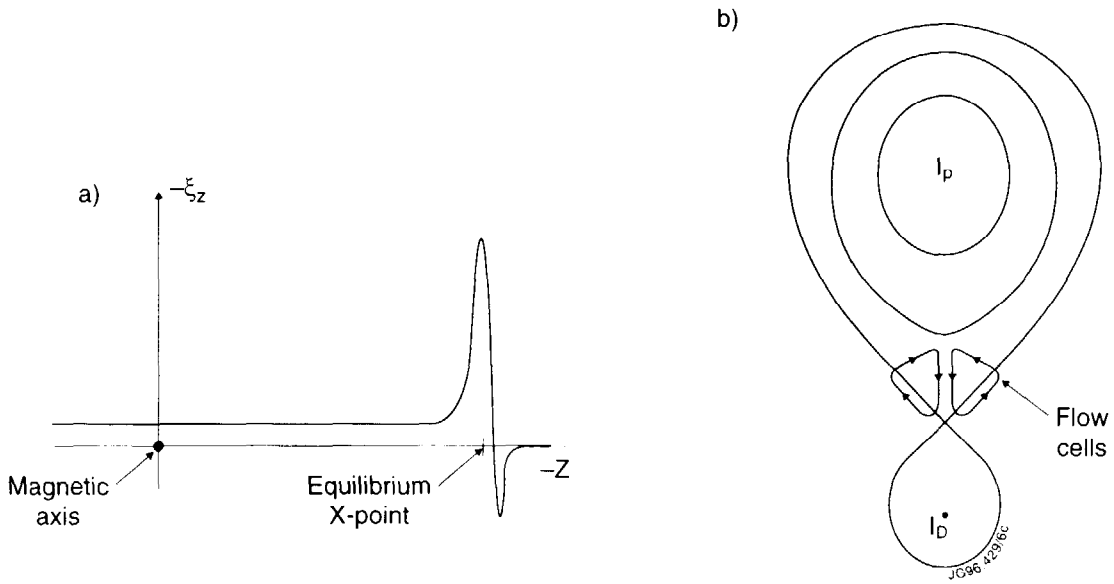

Fig.6: Structure of a non rigid vertical displacement. (a) z-component of the displacement, showing that the non rigidity is localised near the X-point; (b) a sketch of the dominant flow cells in the vicinity of the equilibrium X-point.

The time scale of the instability is

$$\tau_{inst} \sim (\delta / b)^2 \tau_\eta \tag{19}$$

where δ is the width of the layer region where resistive plasma diffusion is important. The determination of δ for experimental comparison requires non-linear considerations. In the linear instability phase, the most relevant regime is likely to yield the classical tearing mode [10] layer width, $\delta \sim (\tau_A/\tau_R)^{2/5}\, b \propto \eta^{2/5}$, and instability growth time, $\tau_{inst} \sim \tau_A^{2/5}\tau_\eta^{3/5} \propto \eta^{-3/5}$. For typical plasma edge parameters on JET, $\tau_{inst} \leq 1$ ms.

Thus, we expect that the X-point plays a very important role in allowing for non-rigid vertical displacements, the non-rigidity being localised near the X-point where resistive diffusion is important. This has two consequences: (i) the non-rigid displacement will drive a current sheet centred at the position of the equilibrium X-point, and (ii) the instability growth time is short owing to the fact that it depends on resistive diffusion in a narrow current layer. Obviously, since only the edge plasma region is significantly affected by the instability, this non-rigid vertical displacement will not lead to a disruption under normal circumstances, but it may play an important role in the physics of ELMs.

We observe that the feedback stabilisation system at JET is not capable of responding promptly to these non-rigid displacements, because of two reasons: (i) the system is set up to react to displacements of the current centroid, which we have seen to be relatively small in our case; (ii) the instability growth time is likely to be smaller than the system response time.

A detailed mathematical derivation of the linearised mode structure will be presented elsewhere. Here, we sketch the main steps. The problem can be treated by standard boundary layer techniques. In the X-point boundary region, the displacement varies rapidly along the (vertical) direction and more slowly along the poloidal direction. Thus, derivatives with respect to the poloidal angle (or the y direction, see Fig. 6a) can be neglected and it will be sufficient to look at the projection over the y=0 plane. The solution in the boundary layer is to be matched asymptotically to the solution in the plasma bulk. This matching procedure will involve a Δ' parameter, defined as in standard tearing mode theory. The novelty of the present calculation is that Δ' will depend on the geometrical parameter D, associated with the external (image) currents, as well as on the equilibrium plasma and divertor current distributions.

4. CONCLUSIONS

At this point, we may ask the question: are non-rigid resistive vertical displacements the cause of ELMs in a toroidal plasma bounded by a magnetic separatrix?

Although this looks like a promising possibility, it is too early to answer the question positively. In fact, even though the considerations in this paper may result in a positive

identification of the relevant forces that drive the ELMs, we are still quite a long way from a satisfactory model for ELMs. In this concluding section, we would like to present a shop list of facts that need to be established yet.

In the first place, as mentioned in the Introduction, the ELM may involve a two-stage process. The first stage may correspond to the growth of a non-rigid vertical displacement and the building up of a current sheet centred about the equilibrium X-point. During this first stage, as long as flux surfaces remain intact, no significant energy release to the wall would occur. The energy relaxation may occur during the second stage triggered by the break up of the current sheet accompanied by broad band magnetic turbulence. This, of course, is a speculation, and the level at which the current sheet becomes unstable requires detailed non-linear analysis. From an experimental point of view, it seems worthwhile to ascertain the existence of two separate stages and the role played by the X-point currents.

Secondly, we would like to define an ELM model, to be implemented in transport codes for reliable plasma simulations. This model should contain a prescription for the onset of ELMs, in other words a practical instability threshold. In all likelihood, the actual threshold will depend on kinetic and collisional processes. It can be expected that refined linear stability analyses will provide relevant information in this respect, as well as indicating possible means of ELM control.

In addition, a satisfactory model should be able to describe the conditions for the occurrence of the different types of ELMs, together with scaling laws for the average ELM repetition frequency.

There is, obviously, still a lot of work to be done.

ACKNOWLEDGEMENTS

The author would like to acknowledge Prof. F. Pegoraro for his introduction to basic MHD processes of X-point magnetic configurations. In addition, the author has benefited from discussions with numerous JET colleagues, in particular: Drs. A. Taroni and J.G. Cordey for motivating discussions, Drs. M. Ottaviani and J.A. Wesson for discussions on the vertical instability, Drs. S. Puppin and F. Milani for discussions on the feedback stabilisation system on JET, Drs. R. Gill, S. Ali-Arshad and J. Lingertat for discussions on the experimental evidence, and M. Romanelli for kindly producing Fig.3.

REFERENCES

[1] H. Zohm, Plasma Phys. Contr. Fusion **38**, 105 (1996).

[2] S. Ali-Arshad et al, EPS Conference, Kiev 1996.

[3] R.D. Gill et al, EPS Conference, Kiev 1996.

[4] J.W. Connor, A Review of Models for ELMs, Report PPN96/20.1, Culham Laboratory, 1996.

[5] S.I. Syrovatsky, Soviet Astron. **10**, 270 (1966).

[6] E.R. Priest, Rep. Prog. Phys. **48**, 955 (1985).

[7] G. Laval, R. Pellat and J.L. Soule, Phys. Fluids **17**, 835 (1974).

[8] J.A. Wesson, Nuclear Fusion **18**, 87 (1978).

[9] M.R. Perrone and J.A. Wesson, Nuclear Fusion **21**, 871 (1981).

[10] H.P. Furth, J. Killeen and M.N. Rosenbluth, Phys. Fluids **6**, 459 (1963).